

LASER PROCESSES FOR THE INDUSTRIAL PRODUCTION OF HIGH EFFICIENCY SILICON SOLAR CELLS

A. Grohe, T. Wütherich, A. Knorz, J. Nekarda, N. Mingirulli, C. Harmel, R. Preu, S. Glunz
Fraunhofer Institute for Solar Energy Systems (ISE), Heidenhofstrasse 2, D-79110 Freiburg i. Breisgau, Germany
Phone: +49 (0)761-4588-5268, Fax: +49 (0)761-4588-9268, E-Mail: andreas.grohe@ise.fraunhofer.de

ABSTRACT: Laser processing of crystalline silicon solar cells has basically been limited to the edge isolation process for standard screen-printed structures. In this paper the potential of some further steps like selective ablation of dielectric layers, ablation of silicon material, laser doping and the generation of laser-fired contacts, which are currently under investigation at Fraunhofer Institute for Solar Energy Systems (ISE) is explained by either theoretical considerations or experimental results. Furthermore, a quick overview over the current laser sources and their applicability in the crystalline silicon solar cell market is given.

Keywords: Laser Processing, Manufacturing and Processing, Selective Emitter

1 INTRODUCTION

Laser processes have penetrated into the crystalline silicon solar market some time ago already, but are currently limited mainly to the process step of laser edge isolation. Few companies use the laser for groove formation or via hole drilling, but the potential of this tool is by far not used appropriately yet. Due to the contactless nature as well as the possibility to process a wide variety of materials with fine structures lasers can be used for a vast field of production steps like ablating, melting and soldering different materials. This paper therefore gives a short overview over some of the most interesting processes under examination at the Fraunhofer Institute for Solar Energy systems (ISE) at the moment. For this purpose these processes are classified according to three groups of primarily processed material (silicon, dielectrics and metals). Subsequently the most interesting ones for every group are explained in further detail.

2 CLASSIFICATION OF LASER PROCESSES

2.1 Applicable laser sources

In this paper we focus on the applicability of laser processes performed by industrially feasible laser sources. Here the working horse in micro material processing definitely is the diode pumped solid state (DPSS) laser. Their fundamental wavelength lies typically in the range of 1064 nm, but frequency conversion is widely used allowing to emit light in the green for frequency doubled (532 nm) and UV (355 nm) for frequency tripled operation. DPSS lasers can emit laser light continuously (continuous wave, cw-operation) but are also often pulsed. The pulse length depends on the hardware setup and can range from ms pulses down to ps. Even though the emitted output power can rise into the kW range in micromachining generally lasers with lower output power in the sub 100 W range are used. Fundamental optics prevents higher powered lasers from achieving good beam qualities which thereupon limits the possibility to focus the energy to small areas. As this frequency conversion is most efficient at high light intensities it is generally applied for short pulse laser sources with pulse lengths in the ns range and shorter.

With these options the DPSS lasers offer a wide field

of processing parameters. Other laser sources may have advantages in specific areas, but generally can not penetrate into the micromachining market due to other limitations. CO₂ lasers for example emit in the deep IR at 10.6 μm. As the possibility to focus depends on the focal length of the lens as well as on the inverse on the wavelength these lasers can not generate spots in the low μm range. Excimer lasers on the other hand deliver very low wavelengths (F₂ produces 157 nm) but require sophisticated beam shaping and delivery optics. In addition to the requirement of undesirable fillings they still fight with the prejudice of being unreliable and hard to handle. Direct diode lasers (800 – 940 nm) offer high output power for a comparatively low price, but generally emit their light continuously (although they can be pulsed as well) and additionally also need sophisticated beam guiding and forming optics in order to make the raw light emission useable. Fiber lasers on the other hand generally are capable of producing almost perfect beam profiles but are limited in their maximum pulse energy due to the damage threshold of the fibers. Nevertheless, all of these lasers might find their niche in the market as soon as it becomes big enough.

Even though laser processing in crystalline silicon solar cell manufacturing currently has its focus on laser edge isolation, many further processes are imaginable. These processes can be classified according to the material the laser has to penetrate.

2.2 Silicon

The major material being processed in all concepts is the wafer material itself. It consists of more or less chemically pure silicon in different crystal formations like the common mono- and multicrystalline wafers as well as few other ones. Despite their different mechanical behavior the optical parameters do not differ significantly, which allows to treat them all identically.

Silicon has always been processed using conventional DPSS lasers. Edge isolation for example is industrially performed by lasers emitting in the fundamental wavelength as well as frequency doubled and tripled.

As can be seen in figure 1 silicon shows reasonable absorption already in the visible wavelength, while wavelengths in the near IR are equivalent with photon energies below the band gap and therefore should not be absorbed well. Reality though behaves different as the

material changes its parameters strongly dependent on heat leading to a reasonable high absorption of near IR in molten Si. This makes a decision regarding the optimal laser parameters very difficult, as effects like focus ability, available output power and cost of ownership have to be regarded in addition to the raw laser material interaction parameters. Nevertheless, currently experiments are underway, whereas the results will be published elsewhere.

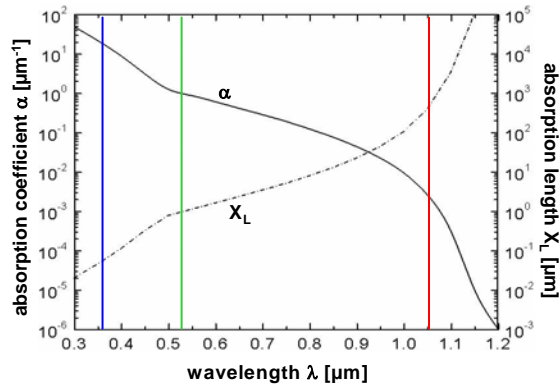


Figure 1: Absorption coefficient α and absorption length X_L over the wavelength for silicon.

2.2 Dielectric materials

The most common dielectric in silicon solar cell production by far is silicon nitride (Si_xN_y), but silicon oxide (Si_xO_y) and silicon carbide (Si_xC_y) have made their way at least into the laboratories as well.

The latter is currently only sparsely used and therefore not covered in this paper. Silicon oxides are generally generated by wet or dry thermal growth which leads to pure SiO_2 , but can also be deposited by means of PECVD. Nevertheless, the absorption of both materials is too low to be machined by conventional DPSS lasers. The rise in absorption below a wavelength of 200 nm can only be reached by F_2 , Xe or ArF excimer lasers. Therefore the direct processing of SiO_2 and Si_xO_y layers also lies behind the scope of this paper.

Silicon nitride as the third material is probably the most common dielectric layer in use so far. In general solar cell production the front side anti-reflection coating (ARC) consists of Si_xN_y layers deposited by sputtering or PECVD (tube or in-line process). Further applications include passivation or diffusion barrier layers for the production of high-efficiency cell concepts. Depending on the purpose common silicon nitride layers generally feature a broad band of refractive indexes n_{SiN} from close to two to more than three, which can be adjusted primarily by the silicon / nitrogen ratio. Furthermore different deposition methods lead to different densities, fine structure, melting points, additives like hydrogen etc. which influence the interaction of the laser process with the layer significantly.

At Fraunhofer ISE we currently focus on the evaluation of ablation processes for two different types of silicon nitrides. One is used as standard ARC and therefore features a low refraction index of $n_{\text{ARC}} \sim 2.1$, the other is a passivating silicon nitride with a higher refraction index $n_{\text{PASS}} \sim 2.8$ which uses the fixed charges in the layer for the generation of a field effect passivation. SiN_{PASS} absorbs light in the visible wavelength range better than silicon. In these cases the

selectivity is easier achievable. Current research furthermore has shown ([1], [2]) that by choosing appropriate laser parameters even SiN_{ARC} , which features a lower absorption than silicon can be processed sufficiently by limiting the damage to a non-relevant level. By selectively ablating the SiN_{ARC} layer from the surface and a subsequent metallization step efficiencies of up to 19.1 % have been achieved. More encouraging as the absolute efficiency value is the fact that the laser processed samples do not lack in efficiency compared to their wet chemically etched counterparts. [2]

2.3 Metals and Alloys

The third big group of materials which need to be processed is already well-investigated due to its close correlation to major laser micromachining fields. In solar cell production so far these metals are limited to a standard assortment consisting of mainly aluminum and silver, but fractions of others like nickel, copper and titanium occur as well. Even though these materials feature wide differences in their thermal parameters like melting and boiling points, chemical reactivity etc. their ability to absorb laser light generally can be treated similar as the fundamental mechanisms are identical. Additionally in solar cell manufacturing generally only thin layers of these metals are penetrated, which leads to a slightly different behavior than for bulk material. Therefore the description of laser processes for metal processing for solar cell applications need to be considered case by case separately and will not be pursued further in this paper, although for example the LFC approach [3] is a very promising technology for the implementation of the passivated emitter and rear (PERC) structure into industrial production lines.

3 LASER PROCESSES IN SOLAR CELL PRODUCTION

Currently the most common cell type for crystalline silicon features screen-printed metallization on front and rear side and therefore the widely known aluminum back surface field (Al-BSF) as rear side passivation and reflector. Although being in use at most cell manufacturers this approach leads to numerous disadvantages over the more sophisticated technologies used in laboratories. The most obvious losses result from:

- high shading losses of front metallization due to poor aspect ratio of $\sim 1:10 \rightarrow$ lower current achievable
- high series resistance due to low contact fraction between front side metal and semiconductor \rightarrow limitations on surface doping concentration in order to achieve good conduction into metallization
- high series resistance within contact grid on front side as screen printing paste conducts only $\frac{1}{2}$ as good as pure metal \rightarrow high cross-section necessary leading to even more shading losses
- low passivation quality of full area alloyed aluminum on rear side \rightarrow higher recombination
- low optical reflectance of rear side metallization for long wavelength range \rightarrow reduced probability of charge carrier generation
- varying heat expansion coefficient leads to wafer bowing during final sintering step \rightarrow high breakage risk and limitation in minimal wafer thickness

- screen printing process depend on mechanical contact of screen with wafer → higher breakage rate

In order to further decrease the costs / Wp novel cell concepts which eliminate or at least reduce these disadvantages are necessary. Those cell structures feature dielectric passivation layers on the rear side for reduced recombination and better optical performance (passivated emitter and rear cell “PERC” concept [4]), improved front side metallization schemes in order to minimize electrical and shading losses or finally the reduction or complete elimination of the front side metallization (metal / emitter wrapped through to the cells rear side using via holes “MWT / EWT” [5]). Even real single (back) side structures are possible. The use of lasers to achieve these goals are manifold, but can be classified in the three groups mentioned in chapter 2, namely silicon, dielectrics and metals.

Silicon is processed in lines for the implementation of laser grooves on the front side for the laser-grooved buried contacts as well as during the edge isolation. Some of the optimized structures feature via holes through the wafer, which are drilled by lasers. Laser doping of selective structures is performed just in the temperature region between melting and boiling point and therefore works without material evaporation. In addition undesired emitter areas can also be selectively removed using laser ablation.

Even though it is possible to ablate silicon with a broad variety of different laser wavelengths as well as pulse lengths, some basic considerations need to be addressed. Generally it is assumed that the photons lead to stimulation of electrons within the material over the band gap to higher states which thus transfer their energy to phonons to drop back to levels close to the band gap. Therefore they contribute strongly to the heating of the material. This makes clear that photon energies lower as the band gap, which is the case for 1064 nm laser light should not be absorbed very well. Nevertheless, effects like impurities, crystal damages and interstitials and eventually more complex processes like multi-photon absorption lead to an initial generation of heat which thus creates more of these absorption centers making the material absorb well in the end as well. Having reached sufficiently high temperatures the bindings break and the material melts and eventually evaporates. This makes clear that no “cold” ablation process can take place when these mechanisms are in place, which is at least for the majority of laser ablation processes with conventional pulse and wave lengths the case.

One important process for further developed solar cell concepts is the generation of via holes in order to produce a possible connection between front and rear side of MWT and EWT cells. This connection gets its conductivity either from metal, which is covering the holes walls or by a doped emitter layer at the surface of the walls. As the conductivity for metal is some magnitudes higher than for doped silicon fewer holes are necessary (100’s instead of 10,000’s) for the MWT cell. Due to the requirements regarding minimal hole diameters the better focusability of lower wavelengths is not necessarily beneficial. Additionally the via hole drilling speed correlates strongly to the energy density as well as the energy distribution over time. Currently this process is performed by DPSS lasers in fundamental

wavelength with high beam quality, fairly long pulses (μs range) and as much pulse energy as possible. Even though lower wavelengths with equivalent power levels might possibly perform better unfortunately there are currently no adequate laser sources available. An example for a via hole generated with the above mentioned laser is shown in figure 2. It was drilled through a 270 μm thick planar Cz silicon wafer using nine pulses per hole and subsequently damage etched to remove the laser damage (see [6]). A taper (aspect ratio of entrance diameter to exit diameter) of approximately 3:1 can be seen which is generally desired for easier diffusion or metallization into the holes.

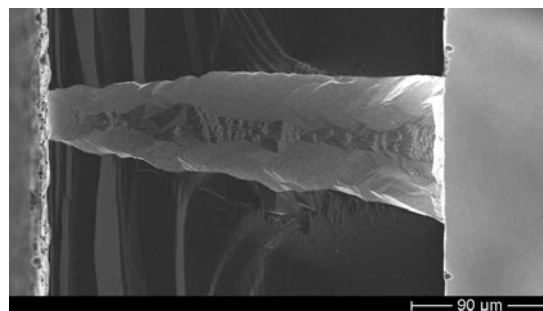


Figure 2: Cross section of a via hole as SEM picture. The beam entry is on the right, the exit on the left.

Laser doping on the other hand is one of the most interesting laser processes evaluated in laboratories at the moment. It allows the generation of single-sided emitter layers which lack the need of overcompensating or removing the rear side residual emitter. Even more beneficial though is the possibility to generate different emitter structures in the lateral dimension, so called selective emitters. They allow to address the specific demands of the different areas individually, namely good metal-semiconductor-contact resistance underneath the metallization and low recombination in the current generating area. Furthermore, the interdigitated grid structure used for back contacted solar cells can be formed much easier. This would further simplify the fabrication process which at our institute is currently based on diffusion barriers (which can be structured by lasers as well). The difference in the emitter profile can be seen in the secondary ion mass spectroscopy (SIMS) profiles in figure 3. As can be seen the shape of the profiles is quite different, as for the laser doped one a broader plateau with high doping close to the solubility limit concentrations is formed.

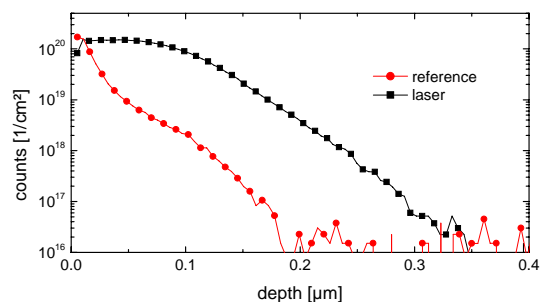


Figure 3: SIMS profiles of a conventional POCl_3 emitter with its typical “kink and tail” shape as well as a laser doped profile with a more homogeneous distribution.

Our primary experiments have shown good results with simplified test structures (see table 1). These 50x50 cm² cells based on 1 Ω cm FZ material feature a homogeneous emitter with various sheet resistances on a planar surface. Underneath the fingers the emitter sheet resistance is lowered to values between 20 and 40 Ω /sq by using a frequency-doubled ns-laser with an optimized beam profile in order to be able to subsequently contact it by a standard screen printing process. The rear side features a conventional screen-printed Al-BSF.

Table 1: Results of the first solar cells being processed using laser doping on planar surfaces. Shown are the best cells with homogeneous as well with selective emitters.

Emitter	V _{OC}	J _{SC}	FF	η
[Ω /sq]	[mV]	[mA/cm ²]	[%]	[%]
90	624	33.1	77.8	16.0
90 / 30	629	32.7	77.5	15.9
150	611	33.3	71.6	14.6
150 / 30	633	32.9	75.5	15.7

As can be seen in table 1 the short circuit current is limited to a value of ~ 33 mA/cm², mainly due to the lack of texture on the front side, increased finger widths in order to align properly and non-optimal rear side reflection due to the polished surface with Al-BSF. By switching to a more efficient rear side structure including an intermediate passivation layer between wafer and metal a gain in open circuit voltage should additionally be possible, as the level of ~ 630 mV is at least partly limited by the low rear side performance. This limit might also be the reason why at least for the samples with 90 Ω /sq emitter no benefit is visible. The 150 Ω /sq emitter nevertheless prove already the principal correctness of the approach as the drop in performance of the homogeneous cell is almost prevented by the selective emitter. Again, the achieved level probably is limited by the structure used.

Another option to achieve selective emitter structures is laser ablation of diffusion barriers. As for this approach two conventional diffusion steps as well as the complete coating and selective opening process needs to be performed we currently prefer the laser doping approach. Nevertheless, for back contacted cells the feasibility of this procedure has been shown already [7]. The more interesting use for a laser ablation process of dielectrics is the front side metallization process. Like already mentioned earlier silicon oxide shows no sufficient absorption in the wavelengths reachable by DPSS lasers. Therefore all our experiments were based on the structuring of silicon nitride layers. They have shown that the influence of the wavelength is more significant than the one of the pulse length, which is the case at least within specific regions. The band gap of a standard ARC silicon nitride with a refractive index of $n_{ARC} \sim 2.1$ corresponds almost perfectly to a wavelength of 355 nm, which predestines frequency-tripled lasers for this purpose. Although ablation of SiN_{PASS} occurs already at 532 nm, even here the use of 355 nm at least provides higher process stability. The potential of this process is shown on 20x20 cm² high efficiency test samples fabricated on 1 Ω cm FZ silicon with a 50 Ω /sq. POCl₃ emitter. They feature a 70 nm thick standard SiN

ARC coating on the planar of textured front side which is selectively ablated using a 355 nm ns-pulsed laser. Front side metallization is realized by a photo lithographically defined and evaporated TiPdAg seed layer thickened by Ag electroplating. The rear side features our standard 105 nm thermally grown SiO₂ passivation layer and 2 μ m of Al contacted by LFC. As is shown in [2] the laser ablated samples match the reference fabricated using photo lithographically defined and wet chemically etched openings in the ARC layer pretty well leading to a maximum efficiency of 19.1 % for the textured and 17.4 % for the planar surface. With optimized emitter profiles this enables to achieve very high efficiency levels with a fairly simple process.

4 CONCLUSIONS AND OUTLOOK

Various industrially feasible laser processes with the potential to further increase the efficiency of crystalline silicon solar cells as well as some underlying considerations for the choice of suited laser sources for these processes were presented. Via hole drilling has always been done by laser usage, but currently the cycle times seem to drop to levels which are low enough for a transfer into industrial environments. Laser doping leads to interesting results within the first run of selective emitter structures, while further adjustments to the sample structure should lead to a future increase of the efficiency and therefore prove the theoretical assumptions. With laser ablation of SiN anti-reflection coatings on high efficiency solar cell structures efficiencies of 19.1 % on textured and 17.4 % on planar surfaces have been shown demonstrating the high potential of this part of a novel metallization technology step as well.

5 ACKNOWLEDGEMENTS

The authors would like to thank all colleagues at Fraunhofer ISE who have contributed to this paper, especially the technical staff in ISE's clean room and PVTEC for their continuous support in providing cells and test structures. Furthermore the possibility to perform experiments with the Edgewave Innoslab Laser is gratefully acknowledged.

6 REFERENCES

- [1] A. Grohe et al, Proc. 21st EU PVSEC (2006),
- [2] A. Knorz et al, Proc. 22nd EU PVSEC (2007), in print
- [3] E. Schneiderlöchner et al, Proc. 17th EU PVSEC (2001), pp. 1303
- [4] A. Blakers et al, Appl. Phys. Let., Vol. 55, pp. 1363
- [5] J.M. Gee et al, Proc. 23rd IEEE PVSC (1993), pp 265
- [6] N. Mingirulli et al, Proc 22nd EU PVSEC (2007), in print
- [7] D. Huljic et al, Proc. 21st EU PVSEC (2006), pp. 765